Local threshold field for dendritic instability in superconducting MgB$_2$ films

F. L. Barkov,[1,2] D. V. Shantsev,[1,3] T. H. Johansen,[1,*] P. E. Goa,[1] W. N. Kang,[4] H. J. Kim,[4] E. M. Choi,[4] and S. I. Lee[4]

[1]*Department of Physics, University of Oslo, P. O. Box 1048 Blindern, 0316 Oslo, Norway*
[2]*Institute of Solid State Physics, Chernogolovka, Moscow Region, 142432, Russia*
[3]*A. F. Ioffe Physico-Technical Institute, Polytekhnicheskaya 26, St. Petersburg 194021, Russia*
[4]*National Creative Research Initiative Center for Superconductivity, Department of Physics, Pohang University of Science and Technology, Pohang 790-784, Republic of Korea*

Using magneto-optical imaging the phenomenon of dendritic flux penetration in superconducting films was studied. Flux dendrites were abruptly formed in a 300-nm-thick film of MgB$_2$ by applying a perpendicular magnetic field. Detailed measurements of flux density distributions show that there exists a local threshold field controlling the nucleation and termination of the dendritic growth. At 4 K the local threshold field is close to 12 mT in this sample, where the critical current density is 10^7 A/cm^2. The dendritic instability in thin films is believed to be of thermomagnetic origin, but the existence of a *local* threshold field and its small value are features that distinctly contrast with the thermomagnetic instability (flux jumps) in bulk superconductors.

I. INTRODUCTION

An abrupt penetration of magnetic flux in the form of branching patterns was observed in 1967, in superconducting Nb alloys.[1] The phenomenon received much attention in the 1990s, when advancements in magneto-optical (MO) imaging allowed studies with a much higher spatial resolution. The branching phenomenon, or dendritic instability, has now been observed in YBa$_2$Cu$_3$O$_7$ films[2,3] (induced by a laser pulse), in field-cooled Nb films,[4] and in zero-field-cooled (ZFC) patterned Nb films.[5] However, the material most sensitive to the instability seems to be the recently discovered superconductor MgB$_2$, a material in which the flux dendrites appear in uniform ZFC films placed in an applied field or triggered by passing a transport current.[6–9]

The dendritic flux instability is believed to be of thermomagnetic origin, similarly to the much further explored phenomenon of flux jumps. Flux jumps are a dominant threat to the stability of the critical state in superconductors, and are especially important in high-current and high-field applications.[10–13] Local heating due to motion of the magnetic vortices reduces the pinning, and will facilitate their further motion. This may lead to an avalanche process, where a macroscopic amount of flux suddenly invades the superconductor—a process accompanied by a strong heating.

A number of common features indicate that the same physical mechanism underlies both the dendritic instability and flux jumps. First, both phenomena occur only at low temperatures, and they develop very quickly (10^4 -10^6 cm/s, see Refs. 1 and 2). Moreover, both instabilities can be suppressed by contacting the superconductor with normal metal so that heat is removed more efficiently.[8,14] Furthermore, dynamics in the form of branching flux and temperature distributions have recently been obtained by computer simulations accounting for the heat produced by flux motion,[6,15] and thus support strongly that the flux dendrites indeed result from a thermomagnetic instability.

There seems to be two necessary conditions for an instability to develop within the dendritic scenario. The first is a small thickness of the superconductor: to our best knowledge, the dendrites have so far been observed only in films with thicknesses $\leqslant 0.5$ μm.[16] The long-range vortex-vortex interactions typical for thin films[17,18] are probably essential for the branching flux structures to form. Secondly, the process should be adiabatic so that the temperature distribution remains highly nonuniform during the dendrite growth. Computer simulations[15] have demonstrated that dendrites occur only when the heat diffusivity is much smaller than the magnetic diffusivity.

The key quantity characterizing flux jump is the applied field, $B_{\rm fj}$, when the first jump occurs in a ZFC superconductor. The $B_{\rm fj}$ also determines the interval between complete flux jumps (the magnetization dropping to zero) as seen in Fig. 1 (left). Therefore, the central question is *whether a threshold field exists also for dendritic flux jumps*. From typical $M(B)$ data for an MgB$_2$ film shown in Fig. 1 (right) the answer seems to be that it does not. The jumps here are very small, typically $\Delta M \sim 10^{-2} M$, because one dendritic structure occupies only a small fraction of the sample. Furthermore, they are irregularly spaced along the applied field axis, and the exact jump pattern is irreproducible when the experiment is repeated.

In the search for a "dendritic" $B_{\rm fj}$ we have performed a magneto-optical study of flux penetration in a virgin MgB$_2$
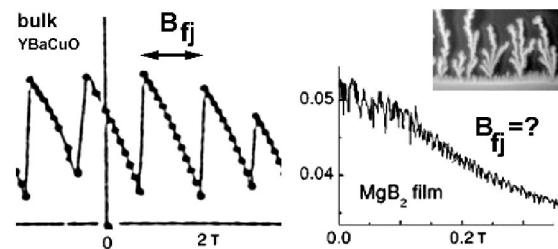
FIG. 1. Magnetization $M(B)$ data exhibiting conventional flux jumps (left, Ref. 19) and irregular small jumps (right, Ref. 20) due to abrupt penetration of flux dendrites shown in the inserted MO image.
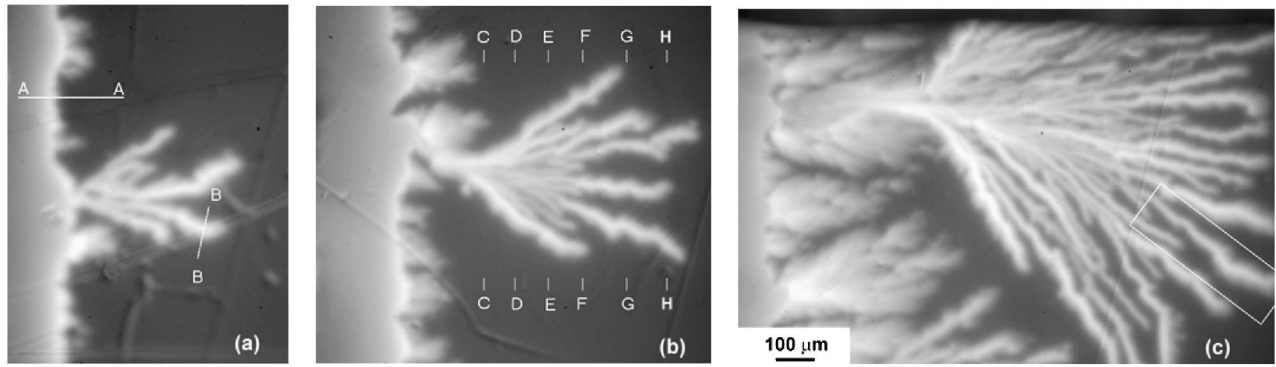
FIG. 2. MO images showing dendritic flux structures formed near the edge of the MgB_2 film at applied fields, which in (a)–(c) are $B_a = 2.3$, 3.2, and 7.4 mT, respectively. The dendritic structures for different B_a differ in size, but not in flux density (image brightness) along the core of the individual branches.

film, and analyzed quantitatively the flux density distributions produced by the dendritic instability. We find that the dendritic instability indeed has a threshold field. However, this is a threshold not for the applied field but instead for the local flux density. This *local* threshold field determines when and where in the superconducting film the dendritic structures nucleate.

The paper is organized as follows. In Sec. II the sample and the experimental method used in this work are briefly described. The results of the MO imaging investigation are presented in Sec. III, and a discussion follows in Sec. IV. Finally, the conclusion is given in Sec. V.

II. EXPERIMENT

Films of MgB_2 were fabricated on Al_2O_3 substrates using pulsed laser deposition.[21] A 300-nm-thick film shaped as a square with dimensions 5×5 mm^2 was selected for the present studies. The sample has a high degree of c-axis alignment perpendicular to the plane, and shows a sharp superconducting transition at $T_c = 39$ K.

The flux density distribution in the superconducting film was visualized using MO imaging based on the Faraday effect in ferrite garnet indicator films. For a recent review of the method, see Ref. 22; description of our setup is found elsewhere.[23] The sample was glued with GE varnish to the cold finger of the optical cryostat, and a piece of MO indicator covering the sample area was placed loosely on top of the MgB_2 film. Before the mounting a few plastic spheres of diameter 3.5 μm were distributed over the sample surface to avoid thermal influence of the MO indicator.

As usual, the gray levels in the MO images were converted to magnetic-field values using a calibration curve obtained above T_c. In all the images shown in the present work, the bright regions correspond to high values of the flux density, while the fully dark areas are free of flux, i.e., Meissner state regions. All the experiments were carried out at $T = 3.6$ K on an initially ZFC sample.

III. RESULTS

The MgB_2 film was placed in a slowly increasing perpendicular applied field, B_a. At small fields, up to $B_a = 2$ mT,

we observed just conventional flux penetration where a gradual increase in B_a results in a smooth advancement of the flux front. Increasing the field further this smooth behavior starts to be accompanied by a sudden invasion of macroscopic dendritic structures, as illustrated in Fig. 2 showing MO images of the flux distribution near the edge at $B_a = 2.3$, 3.2, and 7.4 mT. The images cover different parts of the sample which all have in common that dendritic structures had been formed just before the images were recorded. As in earlier studies, these structures are seen to develop at seemingly random places that vary from one experiment to another, and the dendrites grow to final size faster than we can detect (1 ms). As the applied field continues to increase we find that outside the dendritic areas the flux front advances gradually, while the dendrites that are already formed alway remain completely frozen. Below we will focus on the dendritic flux behavior, and the gradual ''background'' penetration, also displaying interesting nonuniform features, will be the subject of a separate paper.

Let us first look, in a more detailed manner, at one individual branch of a dendritic structure, where the area marked by a white rectangle in Fig. 2(c) was chosen as a typical example. Several flux density profiles across the large branch were measured, with the result seen in Fig. 3. The profiles have an overall triangular shape that varies only slightly along the branch. The maximum flux density in the center remains essentially the same, 10–12 mT, whereas the branch width increases from 30 μm near the root towards 50 μm near the tip. The reason for such broadening is not fully clear, but is probably related to the fact that near the tip the distance from neighboring branches is larger. Near the root of a dendritic structure the branches always grow densely and their mutual repulsion causes each of them to be compressed.

Shown in Fig. 4 is a series of flux density profiles across the whole dendritic ''tree'' seen in Fig. 2(b). To avoid overlap of graphs, subsequent profiles C–H in Fig. 4 are shifted along the vertical axis. By comparing Figs. 2(b) and 4 each peak can be identified as a branch present in the MO image. For profiles C–E in Fig. 4 the outermost branches of the tree are the more pronounced, and many minor ones are located in between. In the profiles F–H in Fig. 4 the number of
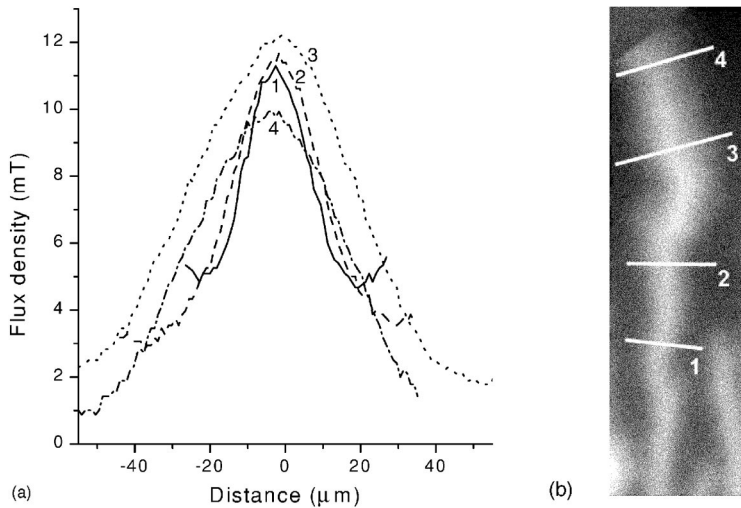
FIG. 3. Profiles of flux density across one branch of a large dendritic structure which appeared at $B_a = 7.4$ mT. The MO image shows the region marked by the rectangle in Fig. 2(c).

branches diminishes, and large flux-free regions exist between them. From this set of curves we see that, like in Fig. 3, the maximum flux density (at the dendrite core) remains essentially constant, $B_{max} \approx 12$ mT, along one branch. Moreover, a striking fact is that this value is the same for all branches.

This universality motivates a comparison also to the B profile across the film edge. Due to demagnetization effects the field becomes concentrated near the edge of a superconducting film, and hence the MO images show a line of maximum brightness exactly along the sample edge. For the comparison we choose the MO image from Fig. 2(a), where the flux penetration near the edge is most regular. The flux density profiles along lines A-A and B-B are presented in Fig. 5. Note that in the A profile of Fig. 5 only the part to the right of the peak is relevant, i.e., representing penetrated magnetic flux. Remarkably, we find that the peak values as well as the slopes of the profiles are essentially the same. Hence, this, together with similar investigations made at other locations, leads us to conclude that the MgB$_2$ film does not allow anywhere in the sample the local field to exceed the value of $B_{max} \approx 12$ mT.

How this universality of B_{max} applies very generally can be illustrated by histograms of the flux density distributions at different applied field. Shown in Fig. 6 are histograms of $B(x,y)$ over the entire field of view of the MO images for three applied fields in the range of 2–8 mT. At 2.3 mT the number of dendrites is small and so is their size, and only a very small fraction of the sample has a local field exceeding 10 mT. As the applied field increases the histogram develops a pronounced peak near 10 mT and the existence of a maximum local field becomes evident. It is clear that although the dendrites that are formed vary widely in their size, and the total area covered by dendrites is very different, the maximum local field remains the same.

IV. DISCUSSION

The existence of the universal field B_{max} sheds new light on the mechanism of dendrite formation. The present results suggest that B_{max} serves as a *local threshold* field for nucle-

ation of the instability. When the ZFC superconducting film is placed in an increasing applied field, its interior remains first flux-free, and the field becomes enhanced at the edges. When the local edge field exceeds B_{max}, an avalanchelike invasion of flux is nucleated there. The avalanche development is then driven not only by local heating, as in bulk superconductors, but in a film also by a local increase of the field. Geometrical field amplification at concave defects along the edge is an effect well known from MO imaging studies,[22,24,25] and is due to the bending of the Meissner currents that are forced to flow around the defected region, in this case the heated spot where the avalanche starts. In the first stage the avalanche grows predominantly in the direction perpendicular to the edge, as seen from the distinct root of the dendritic structures. In a similar way, any perturbation
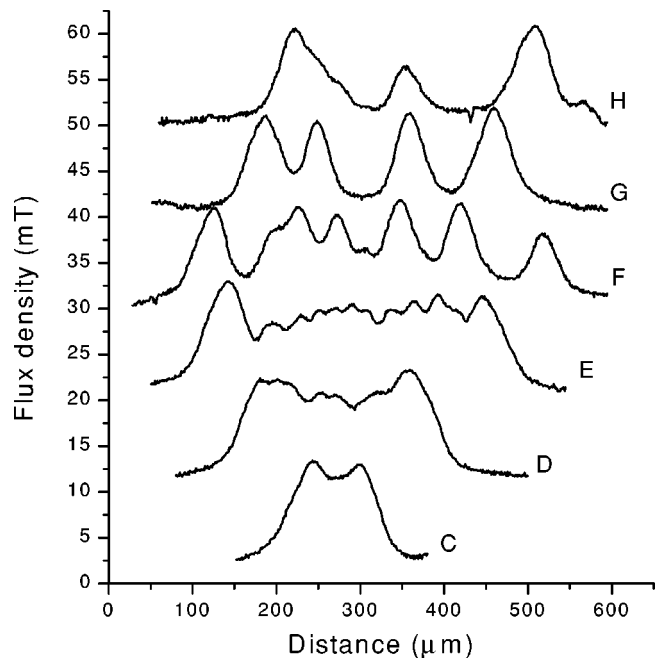
FIG. 4. Flux density profiles across a dendritic structure that appeared at $B_a = 3.2$ mT, shown in Fig. 2(b). To avoid overlap the profiles are shifted (by 10 mT) with respect to each other.
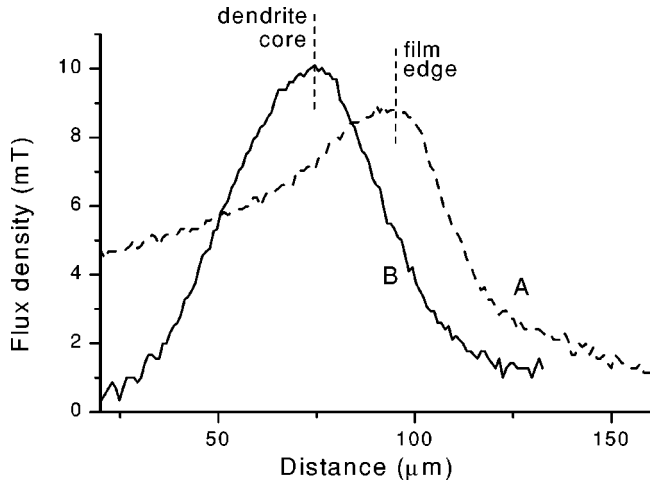
FIG. 5. Profiles of flux density near the edge (A), and across a dendrite (B) obtained from the MO image shown in Fig. 2(a).

along this penetration channel will be enhanced due to the Meissner current bending, and eventually will result in multiple branching. Note that the irreproducibility of the dendritic patterns indicates that the branching points are not directly related to the pinning landscape or other nonuniformities grown into the sample. The dendritic structure will grow and continue branching until the flux density reduces to B_{max} in the cores of all branches. This is the final state of the instability, and it is what we see in the MO images. Upon further increase of the applied field, the condition $B < B_{max}$ soon becomes violated again, now at a different place along the edge from where a new dendritic structure will invade the film.
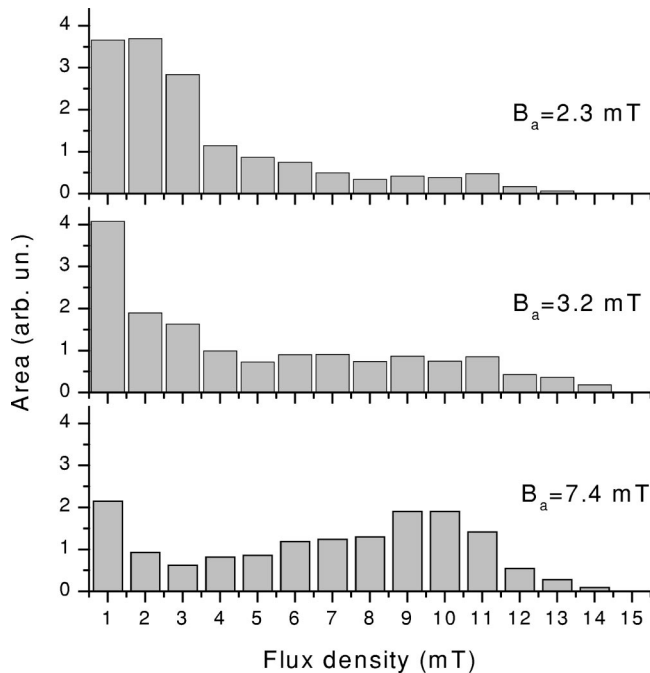
FIG. 6. Histograms of areas having various flux densities (pixel values of the MO images in Fig. 2) in the sample at three applied fields. Despite the quite different B_a all histograms display approximately the same maximum field of 12 mT.

Another interesting result most clearly seen from Fig. 5 is that the slope of the B profiles near the film edge, and across a dendritic branch, is essentially the same. Actually, this slope is also characteristic of all profiles across the large dendritic structure shown in Fig. 4. Since the slopes reflect the local critical current density, j_c, this suggests that they were formed at the same temperature, since j_c is strongly temperature dependent. It is then clear from Fig. 5 that the heating during the dendrite propagation stage was localized to a very narrow core of the branch. The sharpness of the peaked flux profiles shows that the heated core has a width of 15 μm, or less. This is consistent with results obtained also by Bolz *et al.*[26]

The magnitude of the critical current density can be estimated from the profiles of Fig. 5 using the Bean-model formula for a thin strip in a perpendicular field.[27,28] For small fields, the flux penetration depth is given as $\delta = 0.5w(\pi B_a/\mu_0 dj_c)^2$, where w is the strip halfwidth, and d is its thickness. Substituting here $\delta = 30$ μm and $w = 2500$ μm, one obtains $j_c \approx 10^7$ A/cm^2. Unfortunately, this high j_c is compromised by the dendritic instability which largely influences the macroscopic magnetic properties of the film. Magnetization curves of MgB$_2$ films in general are chaaracterized by the following: (i) they contain numerous dips of different magnitudes (noisy behavior) and (ii) the average M recalculated into the critical current density gives a much lower value than the "true" j_c.[20,6]

Let us compare the experimentally found threshold field 12 mT with theoretical estimates. The first jump field, within the adiabatic approach and the Bean model, is given as[10–13]

$$B_{fj} = \left(\frac{2\mu_0 C j_c}{\partial j_c/\partial T} \right)^{1/2}, \quad (1)$$

where C is the heat capacity. This result is obtained for bulk superconductors and should be modified for thin samples in a perpendicular field. Using the Bean-model flux distributions in thin films[27,28] one can show[29] that the field B_{fj} should be multiplied by a factor $\sim \sqrt{d/w}$. Then, substituting $C = 0.3$ kJ/K m^3 (Ref. 30) in Eq. (1), assuming $j_c(T) \propto (T_c - T)$, we obtain $B_{fj} = 1.5$ mT at 4 K. Note that this B_{fj} should give the *applied* field when the first flux dendrite enters a ZFC film. For our experiments on the MgB$_2$ film this field equals 2 mT, in excellent agreement with the theoretical estimate.

At this field, $B_a = 2$ mT, the local flux density was measured to be 12 mT (Fig. 5) at the film edge.[31] After many dendrites have entered the film, the flux distribution became strongly nonuniform, and the criterion for the threshold *applied* field B_{fj} is no longer applicable. Nevertheless, we find that the value 12 mT can still be used as a *local* threshold field.

The penetration scenario has to be slightly modified for a superconductor with initial nonzero uniform flux density $\widetilde{B}$. For conventional flux jumps in bulk superconductors the presence of a frozen-in field leads to a shift of the instability field by $\widetilde{B}$ because only the difference $B_a - \widetilde{B}$ is important. This is readily seen from Fig. 1 (left), where every jump creates almost uniform flux distribution in the sample with

flux density equal to the applied field. A similar shift of the threshold field is also expected for the dendritic instability.

V. CONCLUSIONS

In summary, we have found, using magneto-optical imaging, that the nucleation as well as the termination of dendritic flux avalanches in superconducting MgB_2 films are governed by a local threshold field, $B_{max} \approx 12$ mT. Avalanches nucleate near the edge whenever the local flux density exceeds B_{max} and the flux invasion proceeds as long as there exist regions where $B > B_{max}$. As a result, each avalanche ends with a flux distribution where $B = B_{max}$ in the cores of all branches of the dendritic structure. We find that as the applied field is increased, the flux density at the edge remains equal to B_{max}, while new dendritic flux structures will invade the film. The width of the dendrite cores, which are the heated channels of flux invasion, was found to be 15 μm, or less, whereas in the final state the dendrite fingers are 60–80-μm wide.

*Email address: t.h.johansen@fys.uio.no

[1] M.R. Wertheimer and J. de G. Gilchrist, J. Phys. Chem. Solids **28**, 2509 (1967).

[2] P. Leiderer, J. Boneberg, P. Brüll, V. Bujok, and S. Herminghaus, Phys. Rev. Lett. **71**, 2646 (1993).

[3] U. Bolz, J. Eisenmenger, J. Schiessling, B.-U. Runge, and P. Leiderer, Physica B **284-288**, 757 (2000).

[4] C.A. Duran, P.L. Gammel, R.E. Miller, and D.J. Bishop, Phys. Rev. B **52**, 75 (1995).

[5] V. Vlasko-Vlasov, U. Welp, V. Metlushko, and G.W. Crabtree, Physica C **341-348**, 1281 (2000).

[6] T.H. Johansen, M. Baziljevich, D.V. Shantsev, P.E. Goa, Y.M. Galperin, W.N. Kang, H.J. Kim, E.M. Choi, M.-S. Kim, and S.I. Lee, Europhys. Lett. **59**, 599 (2002).

[7] T.H. Johansen, M. Baziljevich, D.V. Shantsev, P.E. Goa, Y.M. Galperin, W.N. Kang, H.J. Kim, E.M. Choi, M.-S. Kim, amd S.I. Lee, Supercond. Sci. Technol. **14**, 726 (2001).

[8] M. Baziljevich, A.V. Bobyl, D.V. Shantsev, E. Altshuler, T.H. Johansen, and S.I. Lee, Physica C **369**, 93 (2002).

[9] A.V. Bobyl, D.V. Shantsev, T.H. Johansen, W.N. Kang, H.J. Kim, E.M. Choi, and S.I. Lee, Appl. Phys. Lett. **80**, 4588 (2002).

[10] P.S. Swartz and C.P. Bean, J. Appl. Phys. **39**, 4991 (1968).

[11] S.L. Wipf, Phys. Rev. **161**, 404 (1967).

[12] S.L. Wipf, Cryogenics **31**, 936 (1991).

[13] R.G. Mints and A.L. Rakhmanov, Rev. Mod. Phys. **53**, 551 (1981).

[14] R.B. Harrison, J.P. Pendrys, and L.S. Wright, J. Low Temp. Phys. **18**, 113 (1975).

[15] I. Aranson, A. Gurevich, and V. Vinokur, Phys. Rev. Lett. **87**, 067003 (2001).

[16] The only exception is Nb-Zr discs with thicknesses $\geq 0.01-0.1$ mm studied in Ref. 1. The appearance of the flux patterns in this work was also quite different from other studies. (Refs. 2–9).

[17] J. Pearl, Appl. Phys. Lett. **5**, 65 (1964).

[18] E.H. Brandt, Rep. Prog. Phys. **58**, 1465 (1995).

[19] K. Chen, S.W. Hsu, T.L. Chen, S.D. Lan, W.H. Lee, and P.T. Wu, Appl. Phys. Lett. **56**, 2675 (1990).

[20] Z.W. Zhao, S.L. Li, Y.M. Ni, H.P. Yang, Z.Y. Liu, H.H. Wen, W.N. Kang, H.J. Kim, E.M. Choi, and S.I. Lee, Phys. Rev. B **65**, 064512 (2002).

[21] W.N. Kang, H.J. Kim, E.M. Choi, C.U. Jung, and S.I. Lee, Science **292**, 1521 (2001).

[22] Ch. Jooss, J. Albrecht, H. Kuhn, S. Leonhart, and H. Kronmueller, Rep. Prog. Phys. **65**, 651 (2002).

[23] T.H. Johansen, M. Baziljevich, H. Bratsberg, Y. Galperin, P.E. Lindelof, Y. Shen, and P. Vase, Phys. Rev. B **54**, 16 264 (1996).

[24] M.R. Koblischka, *Handbook of Thin Film Materials, Nanomaterials and Magnetic Thin Films*, edited by H. S. Nalwa (Academic, New York, 2002), Vol. 5, Chap. 12.

[25] T.H. Johansen, M. Baziljevich, H. Bratsberg, Y. Shen, P. Vase, and M.E. Gaevski, *High-Temperature Superconductors: Synthesis, Processing and Applications II*, edited by U. Balachandran and P.J. McGinn (Minerals, Metals, & Materials Society, Warrendale, PA, 1997), p. 99.

[26] U. Bolz, B.-U. Runge, and P. Leiderer (private communication).

[27] E.H. Brandt and M. Indenbom, Phys. Rev. B **48**, 12 893 (1993).

[28] E. Zeldov, J.R. Clem, M. McElfresh, and M. Darwin, Phys. Rev. B **49**, 9802 (1994).

[29] M. Daumling and D.C. Larbalestier, Phys. Rev. B **40**, 9350 (1989).

[30] Ch. Wälti, E. Felder, C. Degen, G. Wigger, R. Monnier, B. Delley, and H.R. Ott, Phys. Rev. B **64**, 172515 (2001).

[31] The measured value 12 mT is sensitive to the distance between the MO indicator and the superconducting film, which was ~ 5 μm in the current setup. Measurements directly at the surface would give a slightly larger value, but clearly they would not change the fact that a local threshold field exists.